





Wolf-Hirschhorn syndrome candidate 1 (*Whsc1*) methyltransferase signals via a *Pitx2-miR-23/24* axis to effect tooth development

Received for publication, April 25, 2023, and in revised form, September 1, 2023. Published, Papers in Press, October 6, 2023.

<https://doi.org/10.1016/j.jbc.2023.105324>

Dan Su^{1,2} , Steve Eliason^{1,2}, Zhao Sun³, Fan Shao¹ , and Brad A. Amendt^{1,2,4,*}

From the ¹Department of Anatomy and Cell Biology, and ²Craniofacial Anomalies Research Center, Carver College of Medicine, The University of Iowa, Iowa City, Iowa, USA; ³College of Medicine, Washington University St Louis, St Louis, Missouri, USA; ⁴Iowa Institute for Oral Health Research, College of Dentistry, The University of Iowa, Iowa City, Iowa, USA

Reviewed by members of the JBC Editorial Board. Edited by Brian Strahl

Wolf-Hirschhorn syndrome (WHS) is a developmental disorder attributed to a partial deletion on the short arm of chromosome 4. WHS patients suffer from oral manifestations including cleft lip and palate, hypodontia, and taurodontism. WHS candidate 1 (*WHSC1*) gene is a H3K36-specific methyltransferase that is deleted in every reported case of WHS. Mutation in this gene also results in tooth anomalies in patients. However, the correlation between genetic abnormalities and the tooth anomalies has remained controversial. In our study, we aimed to clarify the role of *WHSC1* in tooth development. We profiled the *Whsc1* expression pattern during mouse incisor and molar development by immunofluorescence staining and found *Whsc1* expression is reduced as tooth development proceeds. Using real-time quantitative reverse transcription PCR, Western blot, chromatin immunoprecipitation, and luciferase assays, we determined that *Whsc1* and *Pitx2*, the initial transcription factor involved in tooth development, positively and reciprocally regulate each other through their gene promoters. miRNAs are known to regulate gene expression posttranscriptionally during development. We previously reported *miR-23a/b* and *miR-24-1/2* were highly expressed in the mature tooth germ. Interestingly, we demonstrate here that these two miRs directly target *Whsc1* and repress its expression. Additionally, this miR cluster is also negatively regulated by *Pitx2*. We show the expression of these two miRs and *Whsc1* are inversely correlated during mouse mandibular development. Taken together, our results provide new insights into the potential role of *Whsc1* in regulating tooth development and a possible molecular mechanism underlying the dental defects in WHS.

Wolf-Hirschhorn syndrome (WHS) is a genetic disorder that is estimated to affect one in 50,000 births. WHS patients show different levels of symptoms which consist of a characteristic facial appearance, delayed growth and development, intellectual disabilities, and seizures (1–5). WHS is caused by subtelomeric deletions of the short arm of chromosome 4 (4p)

and the variety and severity of the clinical features largely depend on the number and roles of the genes in the deletion (6–8). In addition to these common features, delayed tooth development and tooth anomalies have also been considered as underestimated traits with a prevalence of 50% in WHS patients (9–11). WHS candidate 1 (*WHSC1*) or nuclear receptor binding SET domain protein 2 (*NSD2*), is a H3K36-specific methyltransferase (12–15). This gene resides in the “critical region” of WHS and is deleted in every case of WHS (4, 16). Interestingly, it has been reported that patients with nonsense or loss-of-function variant of *WHSC1* also exhibit a subset of WHS features, including intrauterine growth retardation and global developmental delay (17, 18). Interestingly, a patient with *de novo* nonsense mutation in the *WHSC1* gene (c.3412C > T, p.Arg1138Ter, NM_001042424.2) also shows tooth enamel dystrophy (19). *Whsc1*-deficient mice have WHS features including growth retardation, cleft palate, bone defects, congenital heart disease, and malocclusion (15, 20). These reports suggest a potential role of *WHSC1* in regulating tooth development.

Tooth development is a complex process requiring reciprocal interactions between the dental epithelium and mesenchyme, involving bone morphogenetic protein, wingless-related integration site, fibroblast growth factor, and Sonic Hedgehog signaling pathways (21). This cell-cell communication requires rigid spatiotemporal regulation of transcription factors (TFs) to ensure a staged morphogenesis of individual tooth germs (initiation, placode, bud, cap, and bell), as well as odontoblast and ameloblast differentiation, the two unique dental cell types producing dental hard tissues (22). *PITX2* is the earliest TF observed in tooth development, which has long been considered to regulate the transcriptional hierarchy in early stages of tooth development, as well as the stem cell niche (23–28). It controls dental epithelial stem cell activity by activating several genes, including *Lef-1* and *Sox2* and thus initializes embryonic tooth development and enamel formation (29–34).

MicroRNAs (miRNAs/miRs) are posttranscriptional regulators that repress gene expression by binding to their specific binding sites in the 3'UTR region of target mRNAs, and thus regulate biological processes such as cell proliferation,

* For correspondence: Brad A. Amendt, brad-amendt@uiowa.edu.

Whsc1 regulates gene expression during development

apoptosis, and differentiation (35, 36). They also play important roles in the developing tooth (37–41). For example, dental epithelial-specific KO of *Dicer1*, which encodes a miR processing enzyme, leads to severe enamel defects and supernumerary incisors (37). *miR-23-27-24* clusters, including *miR-23a-27a-24-2* (mouse chromosome 8) and *miR-23b-27b-24-1* (mouse chromosome 13), encode *miR-23a/b*, *miR-27a/b* and *miR-24-1/2*, and their expression are associated with bone development (42–44), endocrine homeostasis (45), cell death (46), glutamine metabolism (47), and cancer development (48). We reported that miRs from this cluster are highly expressed in the mouse tooth germ at P0 (37). A Solexa sequencing of miR expression profiles in miniature pigs also revealed the high expression of miRs in the *miR-23-27-24* cluster during tooth development (49). We recently described a role for *miR-23a* and *miR-23b* in regulating *Hmgn2*, a chromatin-associated factor that inhibits Pitx2 protein function, during dental epithelial development (50).

In this report, we aimed to determine if *Whsc1* has a role in regulating tooth development. We hypothesized that *Whsc1* participates in the regulatory network involving TFs and miRNAs during mouse lower incisor development. In this work, we describe a new molecular mechanism for *Whsc1/Nsd2* in regulating mouse tooth development. *Whsc1*, as a methyltransferase, positively regulates the *Pitx2* promoter. The *Whsc1* promoter is also regulated by *Pitx2*. Furthermore, *Whsc1* is directly targeted by *miR-23a/b* and *miR-24-1/2*. The expression of *Whsc1* and *miR-23-27-24* clusters are negatively correlated during development. Interestingly, *miR-23-27-24* clusters are repressed by *Pitx2*, through interaction of the *Pitx2* protein on a distal binding element upstream of the miR clusters.

Significance

While the developmental and protein function of *Whsc1* has been studied, little is known about its specific expression pattern and regulatory role in causing WHS. Our research defines a specific expression and regulatory network between *Whsc1*, *Pitx2*, and miRs encoded by the *miR-23-27-24* cluster in tooth development, which also indicates a potential mechanism underlying tooth anomalies in WHS.

Results

Whsc1 is developmentally regulated and associated with mesenchymal and epithelial progenitor cells in the mouse incisor

We first examined the expression pattern of *Whsc1* during mouse incisor development (Fig. 1). A schematic of the embryonic stages of mouse lower incisor development is shown for reference (Fig. 1A). At the placode stage (E11.5), *Whsc1* is extensively expressed in the mandible and maxilla. It is more restricted to the dental mesenchyme (DM) and dental epithelium in the mandible, while still expressed ubiquitously in the maxilla at the bud stage (E13.5). At the cap stage (E14.5), when the enamel knot (EK) is formed, *Whsc1* expression is limited to the lingual cervical loop, labial cervical loop (LaCL) and the

DM in the lower incisor tooth germ. Later at bell stages (E16.5 and E18.5), *Whsc1* expression decreases over time. At P1, when the mature tooth germ is formed, *Whsc1* expression is further reduced and limited to the transit amplifying zone and some preameloblasts in the LaCL, as well as some dental mesenchymal cells (Fig. 1B). By costaining with *Lef-1*, which marks the EK in the lower incisor tooth germ, we found that *Whsc1* was excluded from the EK (Fig. 1C). EK is generally recognized as a signaling center that controls the growth of the surrounding epithelium and mesenchyme, while it itself contains a group of nondividing cells (51, 52). Previous studies have reported several cell cycle proteins are expressed in the developing lower incisor tooth germ. The expression pattern of *Ki-67* and *cyclin A* is similar to *Whsc1* (53, 54). We also performed immunofluorescence staining of *Whsc1* in the developing first molar and found a similar expression pattern compared to the incisor (Fig. S1, A and B). This specific expression pattern suggests that *Whsc1* may be linked to proliferation. To test this hypothesis, we performed cell proliferation assays with LS-8 and LS-8-*NSD2* cells. Both the 3-(4,5-dimethylthiazol-2-yl)-2,5-diphenyl-2H-tetrazolium bromide (MTT) and cell counting assays demonstrate a role of *Whsc1* in activating proliferation in dental epithelial cells (Fig. S1, C and D).

We next costained *Whsc1* with progenitor cell markers in the P0 (at birth) tooth germ (Fig. 2). We first costained *Whsc1* with *Pitx2*, the first transcription marker observed during tooth development, and found that they colocalize in the LaCL or dental epithelial stem cells (DESCs) (Fig. 2A). Another DESC marker, *Sox2* shows a similar colocalization with *Whsc1* in the DESCs (Fig. 2B). *Gli-1*, a Sonic Hedgehog signaling mediator and a dental mesenchymal stem cell marker (55, 56), colocalizes with *Whsc1* in the DESCs and DM (Fig. 2C). These data together demonstrate that *Whsc1* is associated with the epithelia and mesenchyme progenitor cells.

Whsc1 and *Pitx2* positively and reciprocally regulate their expression

Because *Pitx2* is an early developmental TF and *Whsc1* is expressed in early development, we asked if *Pitx2* regulates *Whsc1* expression. We first established *Pitx2* and *Whsc1* overexpression stable dental epithelial LS-8 cell lines and performed real-time quantitative reverse transcription PCR (RT-qPCR) (Fig. 3A). *Whsc1* mRNA was increased in the LS-8-*Pitx2* stable cell line and surprisingly, *Pitx2* mRNA was increased in the *Whsc1* stable cell line. We confirmed this regulation by transfection of *Pitx2* and *Whsc1* in HEK 293 cells. Thus, *Pitx2* transfection increased *Whsc1* (Multiple myeloma SET domain [MMSET] II and MMSETI) protein and *Whsc1* transfection increased *Pitx2* protein expression, compared to untransformed cells (Fig. 3B).

We next screened the promoter region of the murine *Whsc1* gene and found a *Pitx2* binding site (TAATCC) at -2.7 kb, which is also conserved in humans (Fig. 3C). The 3.7 kb *Whsc1* promoter was cloned in a luciferase reporter, and the overexpression of *Pitx2* expression increased luciferase (luc)

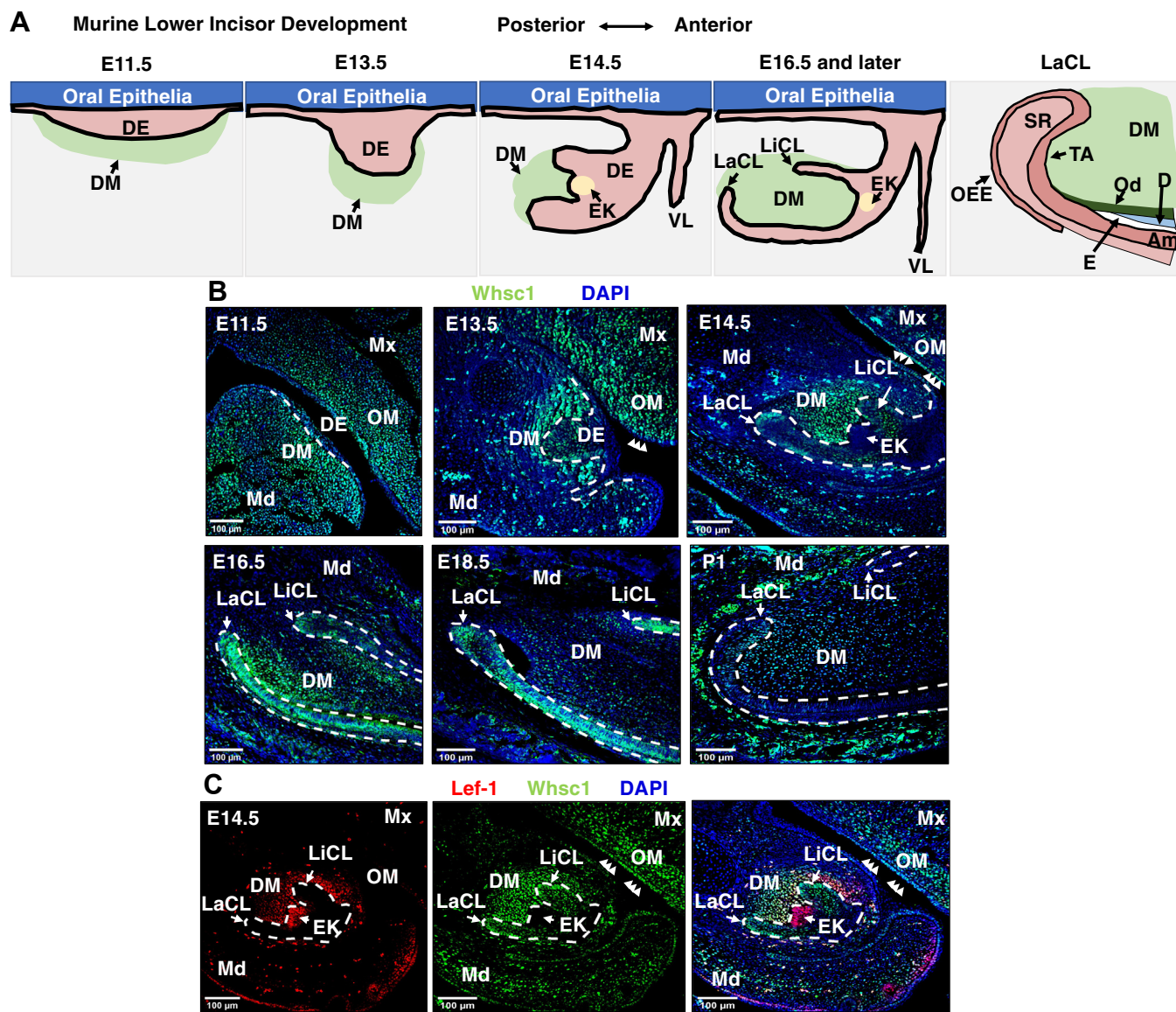


Figure 1. The expression pattern of *Whsc1* during murine lower incisor development. A, *Whsc1* immunofluorescence signal in lower incisors (dental epithelium outlined with *dashes*) at E11.5, E13.5, E14.5, E16.5, E18.5, and P1. DAPI staining represents nuclei. B, representative images showing immunofluorescence staining of *Whsc1* staining from E11.5 to P1. C, representative images showing *Whsc1* and *Lef-1* staining in cap-stage (E14.5) teeth. Regions outlined by *dashes* show cap-stage teeth. *Arrows* indicate *Whsc1* signal in oral epithelial cells and *Lef-1* expression in the EK. The scale bar represents 100 μ m. DAPI, 4',6-diamidino-2-phenylindole; DE, dental epithelium; DM, dental mesenchyme; EK, enamel knot; LaCL, labial cervical loop; LiCL, lingual cervical loop; Md, mandible; Mx, maxilla; OM, oral mesenchyme; *Whsc1*, Wolf-Hirschhorn syndrome candidate 1.

activity 6-fold in cells (Fig. 3C). While *Whsc1* did not increase *Whsc1* promoter luc activity, cotransfection of *Pitx2* and *Whsc1* increased *Whsc1* promoter luc activity at 9-fold compared to control (Fig. 3C). We have previously shown that *Pitx2* autoregulates its expression by binding to a *Pitx2* cis-element in the *Pitx2* promoter (57). We next asked if *Whsc1* could regulate the *Pitx2* promoter. By performing the luciferase assay with the 3 kb *Pitx2* promoter reporter, we show that *Pitx2* or *Whsc1* can upregulate luc activity by 11-fold and 4-fold, respectively (Fig. 3D). Together *Whsc1* and *Pitx2* show an increase in *Pitx2* promoter activity to 14-fold (Fig. 3D). Because *Whsc1* is a methyltransferase that methylates H3K36 in the proximal promoters of genes (12–15, 20), *Whsc1* may activate the *Pitx2* promoter by depositing active

chromatin marks onto its promoter. A chromatin immunoprecipitation (ChIP) assay using a *Pitx2* antibody indicated that *Pitx2* binds to its cis-element in the *Whsc1* promoter (Fig. 3E). Interestingly, the binding of *Pitx2* and *Whsc1* at the *Pitx2* promoter were detected by the ChIP assay (Fig. 3F), suggesting that *Whsc1* is binding to chromatin at the *Pitx2* binding element in the *Pitx2* promoter. Moreover, H3K36me2 is also associated with the *Pitx2* binding sites in the *Pitx2* and *Whsc1* promoters demonstrated by ChIP assays (Fig. S2). In addition, *Whsc1* as well as the H3K36me2 modifications were detected at the *Pitx2* binding element in the *Amelogenin* and *Sox2* promoters (Fig. S3).

Taken together, these data indicate that *Pitx2* upregulates *Whsc1* expression by binding to and activating its promoter;

Whsc1 regulates gene expression during development

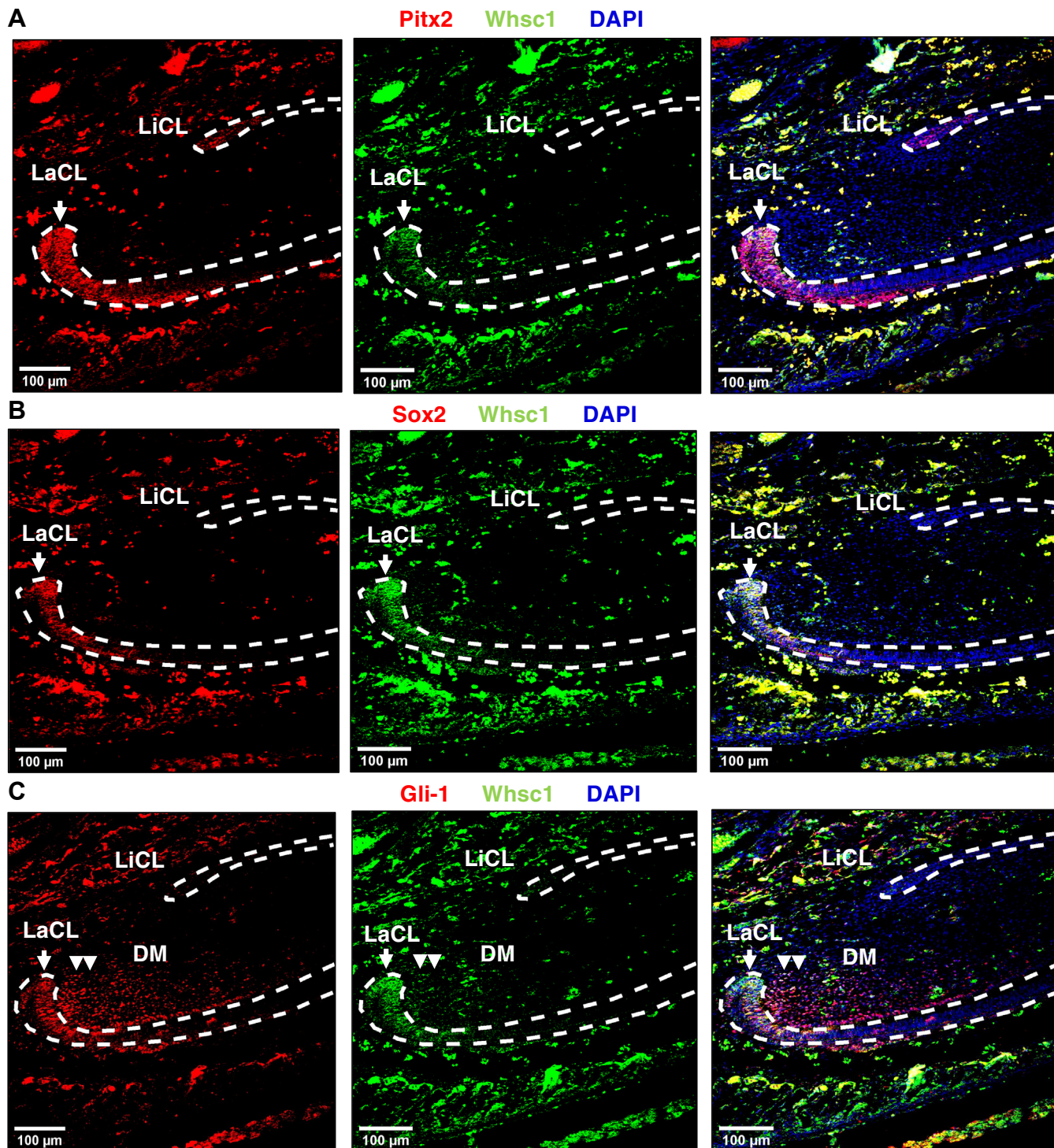


Figure 2. *Whsc1* is expressed in DESCs and DMSCs. A, representative images showing immunofluorescence staining of DESC marker *Pitx2* (Red) and *Whsc1* (Green) in P0 lower incisor. B, representative images showing immunofluorescence staining of DESC marker *Sox2* (Red) and *Whsc1* (Green) in P0 lower incisor. C, representative images showing immunofluorescence staining of DMSC marker *Gli-1* (Red) and *Whsc1* (Green) in P0 lower incisors. The scale bar represents 100 μm. DESC, dental epithelial stem cell; DM, dental mesenchyme; DMSC, dental mesenchymal stem cell; LaCL, labial cervical loop; LiCL, lingual cervical loop; *Whsc1*, Wolf-Hirschhorn syndrome candidate 1.

Whsc1 positively regulates *Pitx2* expression by activating the *Pitx2* promoter, through depositing active chromatin marks around the *Pitx2* proximal promoter. *Whsc1* and *Pitx2* act to positively regulate gene expression through different mechanisms.

***PITX2* represses the expression of the miR-23-27-24 cluster by binding to an upstream distal regulatory element**

miRNAs are known to regulate tooth development. We asked if a discrete group of miRs participates in this *Whsc1*-*Pitx2* regulation of tooth development. Our lab has previously

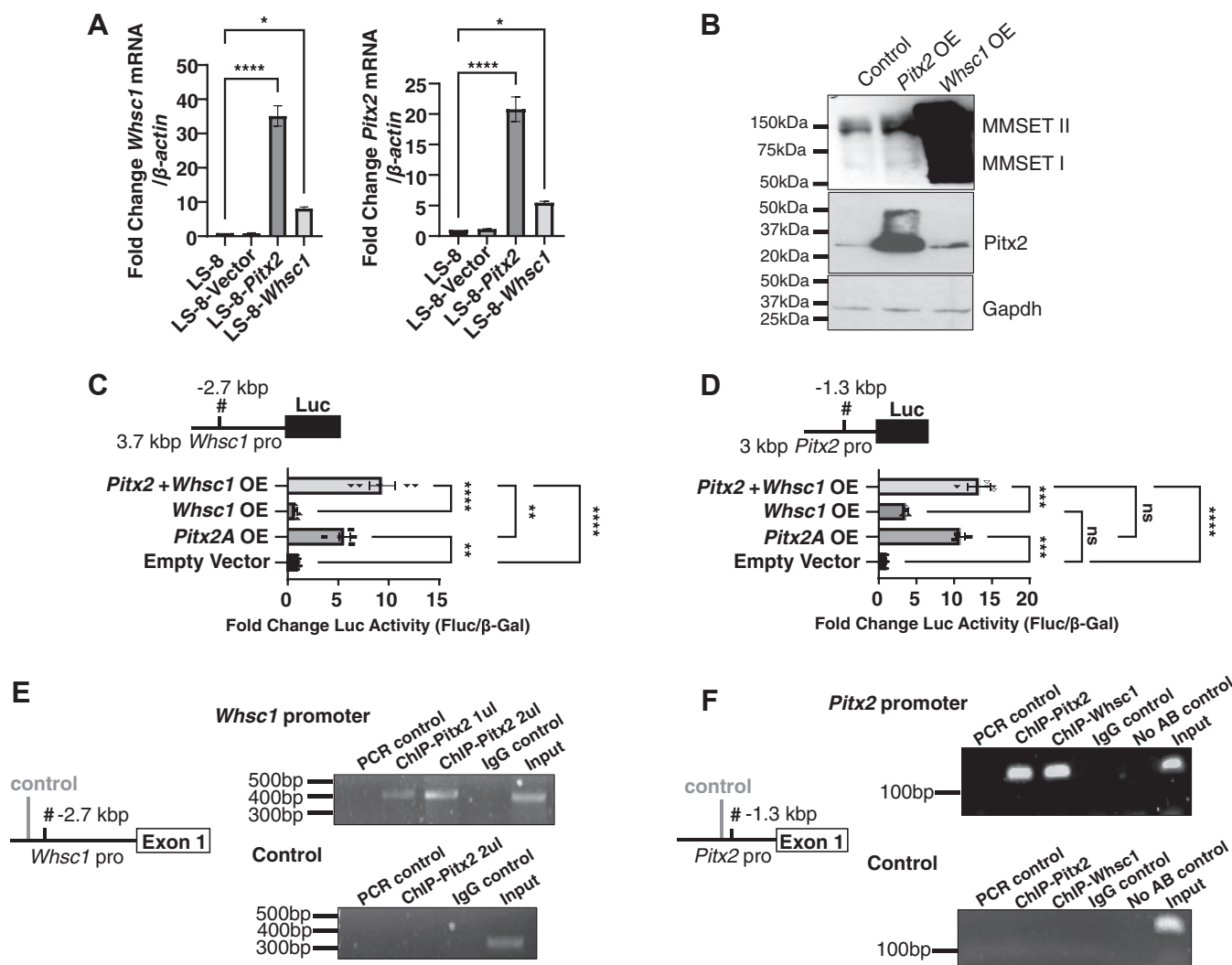


Figure 3. Whsc1 and Pitx2 positively and reciprocally regulate one another. *A*, RNA isolated from the LS-8, LS-8-Vector, LS-8-Pitx2, and LS-8-Whsc1 overexpressing cells were analyzed by qPCR for *Whsc1* and *Pitx2* transcript levels. Relative levels of each transcript are shown (N = 3). *B*, HEK 293T cells were transfected with control, Pitx2 or Whsc1/Nsd2 expression plasmids and proteins were isolated 48 h after transfection. Isolated proteins were then resolved on a 10% SDS-polyacrylamide gel and probed for Pitx2 and two isoforms of Whsc1 (MMSET I and II). Gapdh was used as internal control. The proteins were visualized using ECL reagents. *C* and *D*, LS-8 cells were cotransfected with the *Whsc1* or *Pitx2* luciferase promoter (5 μ g) construct, either Pitx2, Whsc1 or both expression constructs (2.5 μ g). The luciferase activities are shown as mean fold activation compared with the normalized luciferase activity in empty vector (pcDNA 3.1) with the *Whsc1* or *Pitx2* promoter reporter (N = 3–5). *E*, schematic of the *Whsc1* promoter chromatin region and ChIP primers. ChIP assay using anti-PITX2^{ABC} Ab for chromatin immunoprecipitations (IP). Pitx2 bound to the Whsc1 distal element in the Whsc1 promoter. IgG alone did not IP the chromatin. PCR and no AB control groups did not produce a band. Control primers to an upstream region of the *Whsc1* promoter did not detect an IP product in any group except the input. *F*, schematic of the *Pitx2* promoter chromatin region and ChIP primers. ChIP assay using either anti-PITX2^{ABC} or anti-WHSC1 Ab for chromatin immunoprecipitations. Pitx2 and Whsc1 bound to the Pitx2 promoter. IgG alone did not IP the chromatin. PCR and no AB control groups did not produce a band. Control primers to an upstream region of the *Pitx2* promoter did not detect an IP product in any group except the input. #, PITX2 binding site. **p* < 0.05; ***p* < 0.01; ****p* < 0.001; *****p* < 0.0001. ChIP, chromatin immunoprecipitation; IgG, immunoglobulin G; IP, immunoprecipitation; MMSET, multiple myeloma SET domain; qPCR, quantitative PCR; Whsc1, Wolf-Hirschhorn syndrome candidate 1.

performed miRNA arrays in P0 mouse tooth germs and revealed the miR expression profile in the late-stage development of mouse incisors and molars (37). We also performed a miR array in the P0 incisor epithelium of WT and *Pitx2c*^{Tg} mice to detect miRs regulated by Pitx2. Interestingly, we found that miRs from the *miR-23-27-24* cluster (*miR-23a/b*, *miR-24-1/2* and *miR-27a/b*) are highly expressed in both incisors and molars. Moreover, their expressions are downregulated in the P0 incisor epithelium of *Pitx2c*^{Tg} mice (Fig. 4A). We then confirmed that *miR-23a* and *miR-23b* expressions were decreased by Pitx2 in transfected LS-8 cells (Fig. 4B). We found a highly conserved Pitx2 binding site approximately 8.7

kb upstream of the transcription start site (TSS) of *pre-miR-23a-27a-24-2* (Fig. 4, C and D). We performed a ChIP assay with the anti-PITX2 antibody and confirmed the binding of Pitx2 at this specific genomic region (Fig. 4E, see asterisk, and F control). We then cloned a 1 kb region containing the Pitx2 binding element into a luciferase reporter plasmid and performed luciferase assay. The result showed that overexpression of *Pitx2* can repress the luciferase activity from the miR promoter by 50% (Fig. 4G). There is also a highly conserved Pitx2 binding element at 73 kb upstream of *pre-miR-23b-27b-24-1* (Fig. S4, A and B). The binding of Pitx2 at this element was confirmed by ChIP assay (Fig. S4, C and D). These data

Whsc1 regulates gene expression during development

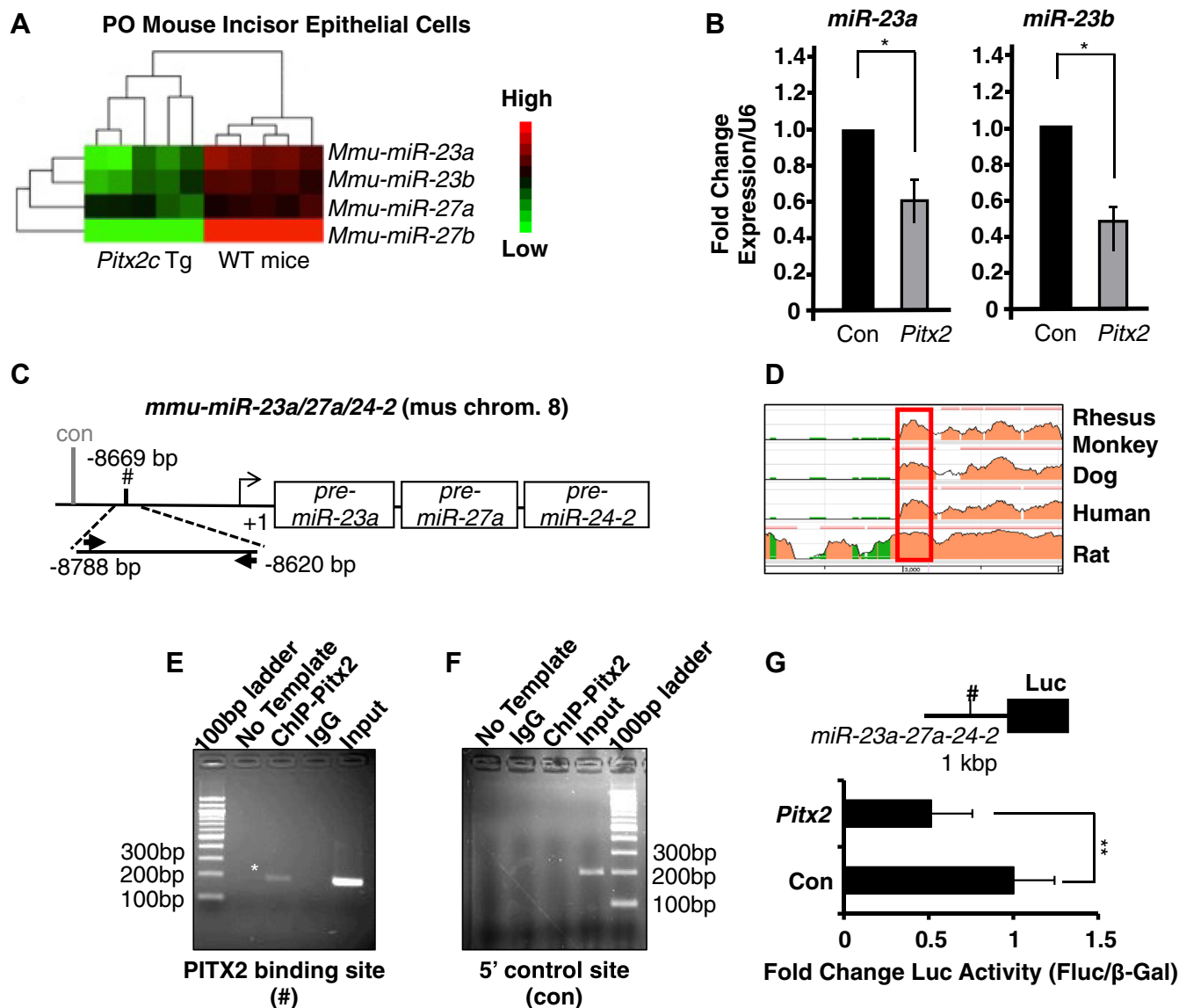


Figure 4. Pitx2 represses *miR-23a* and *miR-23b* expression. *A*, *miR-23a-27a-24-2* and *23b-27b-24-1* cluster expression are down-regulated in *Pitx2c* transgenic mice. microRNA array (heat map) shows the expression levels of *miR-23a/b* families in *Pitx2c*-transgenic and WT P0 mice. *B*, *Pitx2* represses endogenous *miR-23a* and *miR-23b* in epithelial cells. LS-8 cells were cotransfected with 2.5 μ g of either the pcDNA-*Pitx2*, or the empty vector pcDNA3.1 (control) plasmids. The *miR-23a* or *miR-23b* expression levels in cells transfected with *Pitx2* were normalized to cells transfected with empty vector (N = 3). *C*, schematic representation and location of the *Pitx2* binding site in the *pre-miR-23a-27a-24-2* promoter. Pound sign indicates the region containing a conserved *Pitx2* binding element (TCATCC). The gray line (con) indicates a 5' region which lacks *Pitx2* consensus binding motif and was used as negative control. *D*, the *Pitx2* binding element of the mouse *pre-miR-23a-27a-24-2* promoter was mapped to a highly conserved region among mouse, monkey, dog, human, and rat. The red box indicates the PCR amplified region on *pre-miR-23a-27a-24-2* promoter in (C). *E*, ChIP-PCR assay of endogenous *Pitx2* binding to the chromatin region approximately 8600 bp upstream of *pre-miR-23a-27a-24-2* transcript in LS-8 cells. *F*, control ChIP-PCR assay using the *Pitx2* antibody and primers to a 9.9 kb upstream region of the *pre-miR-23a-27a-24-2* transcript. This chromatin region does not contain a *Pitx2* binding site. *G*, inhibition of the *miR-23a-27a-24-2* cluster by *Pitx2*. 1 kb *miR-23a-27a-24-2* enhancer fragment which contains this binding element was cloned into the pTK-Luc reporter vector. LS-8 cells were transfected with 5 μ g *miR-23a-27a-24-2* promoter luciferase reporter constructs. The cells were cotransfected with 2.5 μ g of either the pcDNA-*Pitx2*, or the empty plasmid as a control (pcDNA3.1). Pound sign indicates the region containing a conserved *Pitx2* binding element (TCATCC) (N = 3). * p < 0.05; ** p < 0.01. ChIP, chromatin immunoprecipitation.

indicate that *Pitx2* can repress the expression of tooth-development-related *miR-23-27-24* clusters by interacting with upstream distal regulatory elements.

miR-23a/b and miR-24-1/2 regulate *Whsc1* expression

We analyzed the 3'UTR of the *Whsc1* transcript and observed a conserved binding site for *miR-23a/b-3p* (Fig. 5A). To determine if *miR-23a/b-3p* negatively regulates *Whsc1*

expression, we utilized our previously developed plasmid-based miRNA inhibition system (PMIS) and established stable cell lines that can specifically inhibit *miR-23a/b* expression without affecting *miR-27a/b* or *miR-24-1/2* levels (Fig. S5A). In the PMIS-*miR-23* LS-8 cell line, both mRNA and protein levels of *Whsc1* gene (MMSET I and MMSET II) were elevated (Fig. 5, B and C). By cloning the 3'UTR of *Whsc1* containing either the WT or mutated *miR-23-a/b* binding sites into our luciferase reporter, we found that endogenous *miR-23-a/b* can

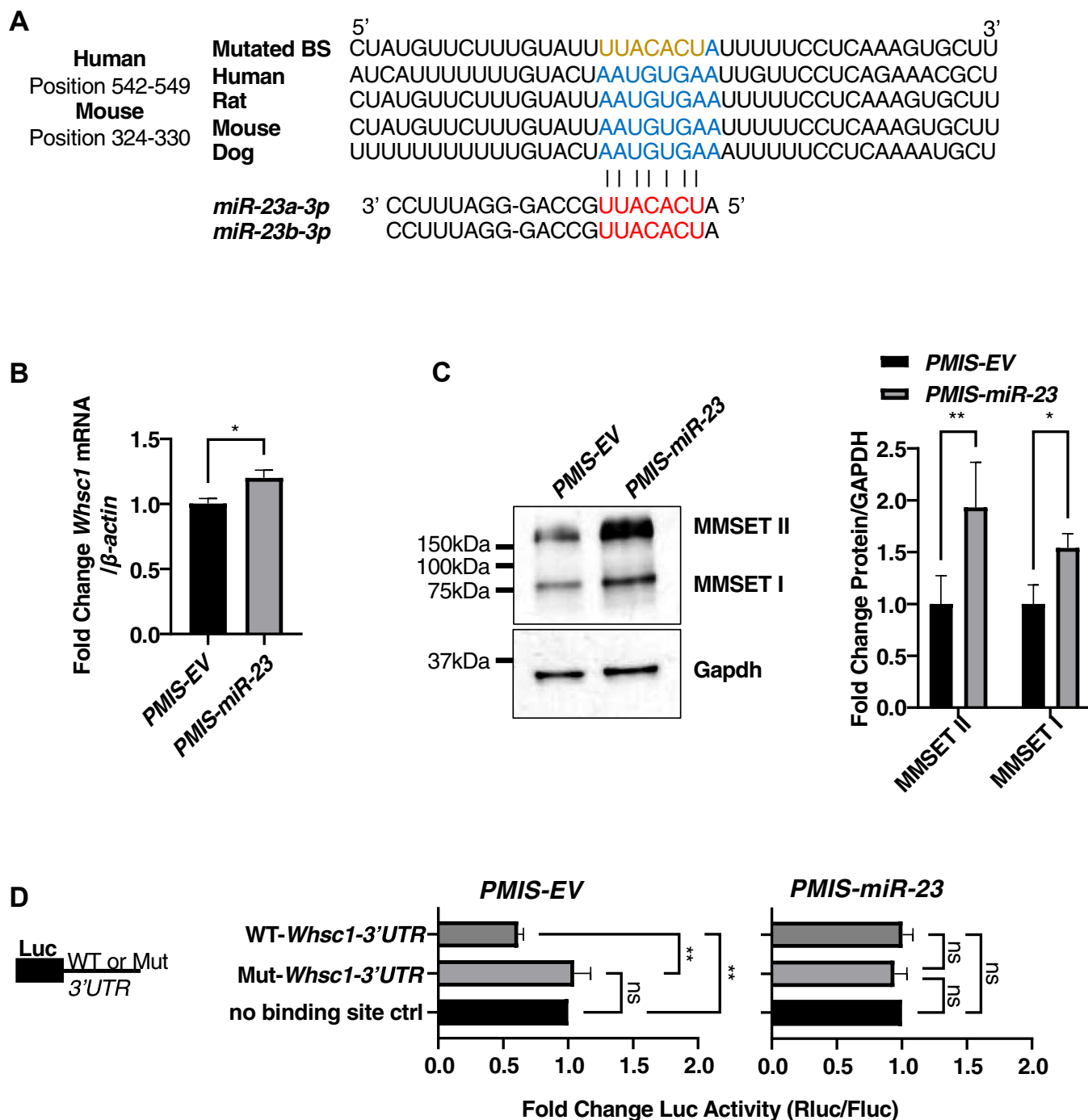


Figure 5. *miR-23a/b-3p* directly targets and inhibits *Whsc1*. *A*, schematics showing the potential *miR-23a/b-3p* binding site in the *Whsc1* 3'UTR, which is highly conserved among different species. Red ribonucleotides represent the seed sequence of *miR-23a/b-3p*; blue ribonucleotides represent the potential binding sites; and gold ribonucleotides represent the mutated binding site used in the luciferase reporter. *B*, RT-qPCR shows *Whsc1* is upregulated in the LS-8-PMIS-*miR-23* stable cell line. The expression of *Whsc1* mRNA is normalized to β -actin. Data are represented as fold change against LS-8-PMIS-EV. *C*, the two main protein isoforms of WHSC1: MMSET I and MMSET II, are upregulated in the LS-8-PMIS-*miR-23* stable cell line. Western blots were quantified using Fiji ImageJ. The band intensity of MMSET I and II were normalized to Gapdh. Data represent the fold change against LS-8-PMIS-EV. *D*, *miR-23a/b-3p* directly targets the WT but not the mutated mouse *Whsc1* 3'UTR. The psiCheck2 reporter with either no binding site control, WT or MT *Whsc1* 3'UTR (5 μ g) were transfected to both LS-8-PMIS-EV and LS-8-PMIS-*miR-23*. Cells were incubated for 48 h and then assayed for Firefly and Renilla luciferase activity (N = 5–7). Data were shown as fold change against no binding site control group. * $p < 0.05$; ** $p < 0.01$. MMSET, multiple myeloma SET domain; Mut, mutant; PMIS, plasmid-based miRNA inhibition system; RT-qPCR, real-time quantitative reverse transcription PCR; Whsc1, Wolf-Hirschhorn syndrome candidate 1.

only bind to the WT 3'UTR to reduce luciferase activity (50%) in the PMIS-EV LS-8 cell line (Fig. 5D). However, this inhibition can be recovered when endogenous *miR-23-a/b* was inhibited by PMIS-*miR-23* in the LS-8 cell line (Fig. 5D).

miR-24-1/2-3p, a miRNA from the same cluster as *miR-23-a/b* also targets *Whsc1* (Fig. 6A). PMIS-*miR-24* LS-8 cell line specifically inhibits *miR-24-1/2* without affecting *miR-23-a/b* or *miR-27-a/b* (Fig. S5B). Both mRNA and protein levels of

Whsc1 regulates gene expression during development

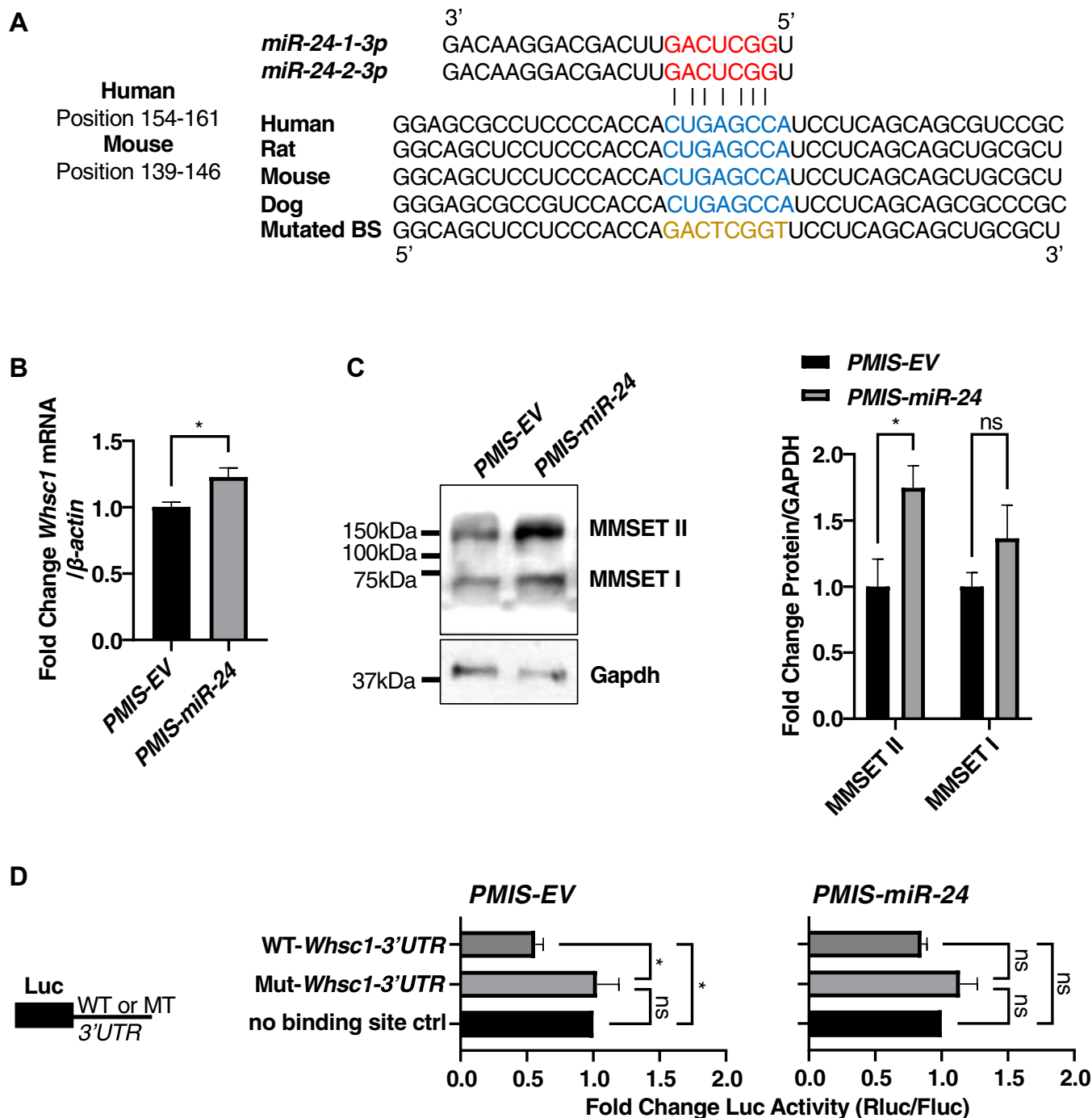


Figure 6. *miR-24-1/2-3p* directly targets and inhibits *Whsc1*. A, schematics showing the potential *miR-24-1/2-3p* binding sites in the *Whsc1* 3'UTR, which are highly conserved among different species. Red ribonucleotides represent the seed sequence of *miR-24-1/2-3p*; blue ribonucleotides represent the potential binding sites; and gold ribonucleotides represent the mutated binding site used in the luciferase reporter. B, RT-qPCR shows *Whsc1* is upregulated in the LS-8-PMIS-*miR-24* stable cell line. The expression of *Whsc1* mRNA is normalized to β -actin. Data are represented as fold change against LS-8-PMIS-EV. C, the two main protein isoforms of WHSC1; MMSET I, and MMSET II are upregulated in the LS-8-PMIS-*miR-24* stable cell line. Western blots were quantified using Fiji ImageJ. The band intensity of MMSET I and II were normalized to Gapdh. Data represent the fold change against LS-8-PMIS-EV. D, *miR-24-1/2-3p* directly targets the WT but not the mutated mouse *Whsc1* 3'UTR. The psiCheck2 reporter with either no binding site control, WT or Mut *Whsc1* 3'UTR (5 μ g) were transfected to both LS-8-PMIS-EV and LS-8-PMIS-*miR-24*. Cells were incubated for 48 h and then assayed for Firefly and Renilla Luciferase activity (N = 5). Data were shown as fold change against no binding site control group. * $p < 0.05$. BS, binding site; MMSET, multiple myeloma SET domain; Mut, mutant; PMIS, plasmid-based miRNA inhibition system; RT-qPCR, real-time quantitative reverse transcription PCR; Whsc1, Wolf-Hirschhorn syndrome candidate 1.

Whsc1 were upregulated upon *miR-24-1/2* inhibition of *miR-24* (Fig. 6, B and C). We also confirmed that endogenous *miR-24-1/2* can decrease the *Whsc1* 3'UTR reporter luciferase activity (~50%) by binding to the WT 3'UTR in PMIS-EV

LS-8 cell line, while inhibition of *miR-24-1/2* recovers the luciferase activity in the PMIS-*miR-24* LS-8 cell line (Fig. 6D). Whsc1 is a histone methyltransferase that deposits methyl groups to histones to maintain open chromatin (12–15). To

assess if the function of the Whsc1 protein was affected by *miR-23-a/b* or *miR-24-1/2*, we performed Western blotting and found the expression of total H3K36me1 and H3K36me2 were increased by *miR-23-a/b* inhibition or *miR-24-1/2* inhibition (Fig. S6).

Endogenous *Whsc1*, *miR-23-a/b*, and *miR-24-1/2* expression were analyzed during murine mandible/tooth development. Mandibular RNA, including incisor and molar RNA, was collected during key tooth development stages (E11.5, E13.5, E14.5, E16.5, E18.5, and P1) and gene/miR expression was assessed by RT-qPCR. The result showed that *Whsc1* decreased while *miR-23-a/b* and *miR-24-1/2* expression increased, which correlates with the expression pattern of *Whsc1* in Figure 1 and Fig. S1 (Fig. 7). These data suggest that *miR-23-a/b* and *miR-24-1/2* directly target and negatively regulate *Whsc1* during embryonic development. The expression of *Whsc1* is negatively correlated with *miR-23-a/b* and *miR-24-1/2* during mandible/tooth development.

Discussion

Epigenetic regulation of gene expression during development is fundamental to tissue and organ specific development. These processes have been well-documented and provide a level of gene expression control that supports cell proliferation and differentiation (58–61). Epigenetic dysfunction is associated with cancer and developmental anomalies such as WHSC1 (MMSET/NSD2) (62). miRNAs regulate gene expression posttranscriptionally and combined with epigenetic factors they offer a mechanism to spatially and temporarily modulate gene expression during different cell processes such as transcription and translation (63). In this report, we have identified a new gene expression regulatory mechanism where *Whsc1*, a methyltransferase, modulates H3K36 at proximal promoters. However, *Whsc1* expression is also regulated by *miR-23a/b* and *miR-24-1/2*. We demonstrate new mechanisms for *Whsc1* in regulating murine tooth development (Fig. 8).

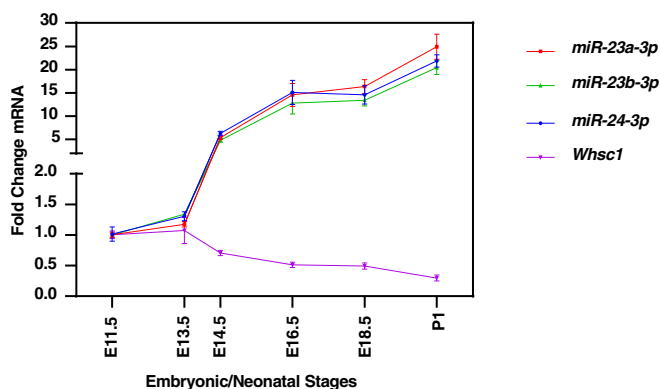


Figure 7. *Whsc1* negatively correlates with *miR-23-3p* and *miR-24-3p* expression during tooth development. Mouse embryos were harvested at different stages during tooth development. The mandibular RNAs were collected and used for qRT-PCR. The *miR-23a/b* or *miR-24-1/2* expression levels were normalized to *U6* and *Whsc1* expression was normalized to β -actin. Data at later time points were represented as fold change against E11.5 (N = 3). qRT-PCR, quantitative real-time PCR; Whsc1, Wolf-Hirschhorn syndrome candidate 1.

Whsc1 regulates tooth development and underlying mechanisms of tooth anomalies in WHS

Tooth anomalies are an underrepresented feature of WHS, with a prevalence of 50% among WHS patients. A candidate gene Msh Homeobox 1 (*MSX1*), which is located 4.9 Mb from the telomere of 4p short arm, is highly associated with tooth agenesis in WHS, including oligodontia (10, 64). However, patients with small deletions (less than 3 Mb) were also found exhibiting delayed tooth eruption and oligodontia, indicating alternative mechanisms underlying the tooth agenesis in WHS (65, 66). *WHSC1* is deleted from every case of WHS. We have demonstrated that *Whsc1* is expressed in the mouse developing tooth germ, and its expression becomes more restricted during embryonic development. At birth (P0) *Whsc1* expression is localized within the LaCL or dental epithelial stem cells and the adjacent DM stem cell region and transient amplifying cells of the lower incisor. These expression profiles suggest that *Whsc1* regulates a progenitor cell niche at later stages of tooth development and associated with undifferentiated cell types.

PITX2 is associated with Axenfeld-Rieger syndrome (ARS), a rare autosomal dominant disorder characterized by a series of craniofacial malfunctions primarily affecting the eye and tooth (23, 24). This novel mechanism of *Whsc1* and *Pitx2* reported in this article has not only broadened our understanding of WHS but has also extended its implications to ARS. Moreover, it also indicates that a potential shared pathway or regulatory network that may contribute to the manifestation of WHS, giving further insights to the etiology of both WHS and ARS.

Whsc1 is associated with proliferating cells in the tooth germ

We show that at E14.5 *Whsc1* is expressed in both LaCL and lingual cervical loop epithelial cells but excluded from the EK, which contains cells that are nonproliferative and apoptotic (67, 68). This expression pattern is identical to that of several cell cycle markers, including Ki67 and cyclin A (53, 54). Our cell proliferation assay indicates that *Whsc1* activates dental epithelial cell proliferation. *Whsc1* has also been reported to positively regulate cell proliferation (69–71). These findings demonstrate a potential role of *Whsc1* in controlling cell proliferation during tooth development.

Whsc1 expression is controlled by miRNAs

Whsc1 expression begins at the early stage of mouse embryogenesis and decreases during development. In the mature incisor tooth germ at P0, *Whsc1* expression is restricted to the *Sox2*⁺ cells in the LaCL and *Gli-1*⁺ cells in the surrounding mesenchyme. The spatial-temporal regulation of gene expression during tooth development is also known to be regulated by miRNAs. We have shown that *Whsc1* is directly targeted by *miR-23a/b* and *miR-24-1/2*. The expression of *miR-23a/b* and *miR-24-1/2* increases as tooth development proceeds, which negatively correlated with the expression of *Whsc1*. According to the previous microarray, *miR-23b* is highly expressed in both the mouse P0 incisor epithelium and

Whsc1 regulates gene expression during development

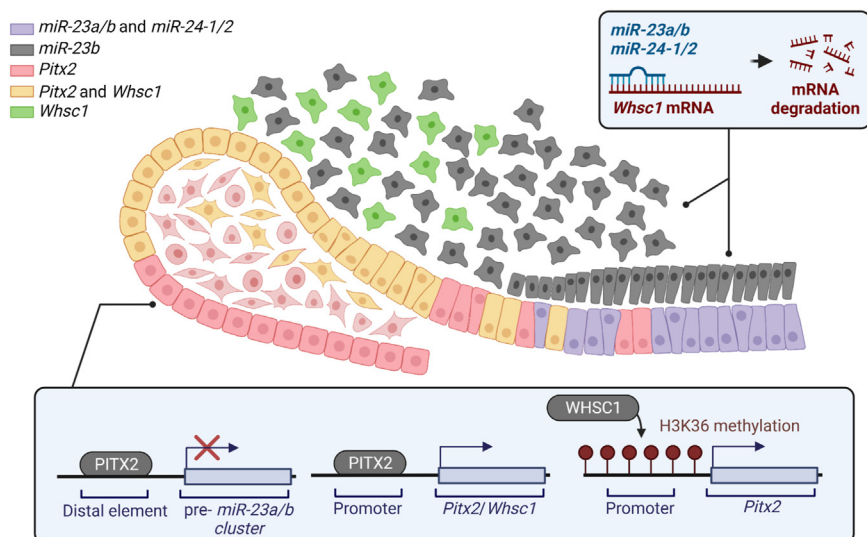


Figure 8. Model for the role of *Whsc1*, *Pitx2*, *miR-23a/b*, and *miR-24* in the regulation of tooth development. In the postnatal mouse lower incisor, *Whsc1* is coexpressed with *Pitx2*, in the LaCL, the transit amplifying zone of inner enamel epithelium, and stellate reticulum. In the *Whsc1*⁺/*Pitx2*⁺ epithelial cells, *Pitx2* activates *Whsc1* expression by binding to its promoter, but inhibits *miR-23/27/24* cluster expression by binding to its enhancer; *Whsc1* activates the *Pitx2* promoter by depositing the active chromatin mark H3K36me1. In the dental mesenchyme, *Whsc1* is also expressed in the *Gli-1*⁺ dental mesenchymal stem cells. *miR-23a/b* and *miR-24-1/2* are expressed in the more differentiated dental mesenchyme and epithelial cells, with *miR-23b* expressed in the mesenchyme and all of them expressed in the epithelium (37). In those cells, *miR-23a/b* and *miR-24-1/2* bind to the 3'-UTR regions of *Whsc1* and inhibit its expression and function. LaCL, labial cervical loop; Whsc1, Wolf-Hirschhorn syndrome candidate 1.

mesenchyme, while *miR-23a* and *miR-24* are more enriched in the epithelium (37). We recently reported that *miR-23a/b* regulates ameloblast differentiation by targeting *Hmgn2* to inhibit its function (50). *Hmgn2* is a chromatin-associated high mobility group protein that binds chromatin and modulates transcriptional activity (72). *Hmgn2* inhibits several TFs from binding DNA and this prevents the activation of gene expression. These data demonstrate a new mechanism where *miR-23a/b* and *miR-24* are expressed in the more differentiated cell types in the tooth germ, which controls the ameloblast and odontoblast differentiation through epigenetic factors.

The role of *Whsc1* in regulating gene expression

Whsc1, also known as *Nsd2*, encodes a H3K36-specific methyltransferase. This chromatin marker is highly associated with open chromatin, which is mostly enriched in the proximity to the TSS of a gene and recruits RNA Pol II machinery to activate transcription (12, 13). It has been reported that *Whsc1* collaborates with TFs to fine-tune the expression of the downstream targets, in regulating heart and bone development (15, 20). We show new roles for *Whsc1* in regulating the *Pitx2* promoter and its downstream targets *Sox2* and *Amelogenin*. Interestingly, we did not observe a direct interaction between *Whsc1* and *Pitx2* (data not shown), which indicates an indirect interaction between these two proteins or alternatively, an indirect regulatory relationship between these two genes. There are genes that have been reported to interact with the *Pitx2* protein and activate its DNA binding and transcriptional activity (31, 32, 73–75). *Whsc1* could activate *Pitx2* through chromatin modulation at the *Pitx2* proximal promoter, or *Whsc1* can activate the expression of gene(s) that can increase *Pitx2* transactivation activity.

In summary, in the postnatal mouse lower incisor, *Whsc1* is coexpressed with *Pitx2*, a dental epithelial stem cell marker, in the transit amplifying zone of inner enamel epithelium, stellate reticulum, as well as some pre-ameloblasts in the LaCL. In the *Whsc1*⁺/*Pitx2*⁺ epithelial cells, *Pitx2* activates *Whsc1* expression by binding to its promoter, but inhibits *miR-23/27/24* cluster expression by binding to its distal regulatory element; *Whsc1* activates the *Pitx2* promoter by depositing the active chromatin mark H3K36me1/2. In the dental mesenchyme, *Whsc1* is also expressed in the *Gli-1*⁺ dental mesenchymal stem cells. *miR-23a/b* and *miR-24-1/2* are expressed in the more differentiated DM and epithelial cells, with *miR-23b* expressed in the mesenchyme and all of the *miR-23/27/24* cluster is expressed in the epithelium (37). In those cells *miR-23a/b* and *miR-24-1/2* bind to the 3'-UTR regions of *Whsc1* and inhibit its expression and function. Thus, we show how *Whsc1* is required for early progenitor cell propagation and the later expression of *miR-23a/b* and *miR-24-1/2* is required for cell differentiation by reducing *Whsc1* expression.

Experimental procedures

Mouse strain breeding and embryonic staging

All animals were housed, and all procedures performed in accordance with the guidelines approved by the University of Iowa Office of Animal Care. All experimental procedures were approved in accordance with the University of Iowa IACUC guidelines. For embryonic staging experiments, the observed vaginal plug date of the female was designated as E0.5. Embryos were collected at the required time point. Embryos were subjected to tissue fixation or mandibular RNA extraction right after harvesting. The *Krt14-PITX2C* transgenic line has been described previously (76).

Immunofluorescence staining and histology

Murine embryos and postnatal pups were fixed in 4% paraformaldehyde (ChemCruz, Santa Cruz Biotechnology) and taken through a standard dehydration before being embedded in the paraffin. Samples were sectioned at 7 μ m with a Thermo (HM325) microtome as previously reported (33). Sections were subjected to standard H&E staining protocols. Slides with paraffin sections were subjected to a series of dewaxing and rehydration steps and then followed by citric acid antigen retrieval in a 100 °C water bath for 12 min. The slides were then blocked with 20% donkey serum and incubated with primary antibodies overnight at 4 °C. Slides were washed with 1xPBS, incubated with Alexa Fluor 488 and 594 secondary antibodies (Thermo Fisher Scientific), and stained with 4',6-diamidino-2-phenylindole. Confocal pictures were taken with a ZEISS 700 confocal microscope and Zen imaging software. The primary antibodies are listed in Table 1.

Expression and luciferase reporter constructs

A 3.7 kb DNA fragment including the PITX2 binding site upstream of mouse *Whsc1* TSS was cloned into the pTK-Luc vector using primers 5'-TAAGCAGGGATCCGATCTG-GAGTCCTGTTTAAT-3', 5'-TGCTTTAGCGATATCTCTAGCCTCTAGGGG-3', 5'-TAAGCAGGATATCAGATCTTCCCAAATCAGATCT-3' and 5'-TGCTTTAGCAAGCTTC-CAGCCTAGATCCTTTGG-3'; this vector construct uses the minimal TK promoter (73). A 1 kb DNA fragment containing the PITX2 binding site upstream of either the *miR-23a-27a-24-2* cluster, or the *miR-23b-27b-24-1* cluster was cloned into the pTK-Luc vector. A luciferase reporter plasmid containing the 3 kb DNA fragment upstream of mouse *Pitx2* was used for luciferase assays as previously described (57).

A 60bp-long DNA fragment of the *Whsc1* 3'UTR containing either WT (5'-AATGTGA-3') or mutant (5'-TCACATT-3') *miR-23-a/b-3p* binding site was ligated downstream of a Renilla luciferase gene in psiCHECK-2 Vector (Promega). A 60bp-long DNA fragment of *Whsc1* 3'UTR containing either WT (5'-CTGAGCC-3') or mutant (5'-GGCTCAG-3') *miR-24-1/2-3p* binding site was ligated downstream of a Renilla luciferase gene in psiCHECK-2 Vector (Promega).

Pitx2 expression construct has been previously reported (31, 32, 50, 76–79). *Whsc1/Nsd2* expression construct (LVXN-Neo-NSD2) was a gift from Darrin Stuart (Addgene plasmid # 86010; <http://n2t.net/addgene:86010>; RRID:Addgene_86010) (80). All the cloned constructs were confirmed by DNA

sequencing. All plasmids used for transfection were purified by double-banding in CsCL.

Our PMIS inhibitor constructs *PMIS-miR-23* and *PMIS-miR-24* were cloned as previously described (81).

Cell culture, transfections, and reporter assays

LS-8 (82), and HEK 293 cells were cultured in Dulbecco's modified Eagle's medium (DMEM) supplemented with 10% fetal bovine serum (FBS) and 1% penicillin/streptomycin. *PITX2*, *WHSC1/NSD2*, *PMIS-EV*, *PMIS-miR-23*, and *PMIS-miR-24* expression plasmids were transfected into LS-8 or HEK 293 cells by either PEI or Lipofectamine 2000 (Invitrogen) reagents, followed by RT-qPCR and Western blot assays. For luciferase reporter assays, cells were seeded 24 h before transfection in 60 mm petri dishes and transfected with 2.5 μ g of expression plasmid, 5 μ g of reporter plasmid and 0.2 μ g of SV-40 β -galactosidase plasmid. Cell transfections were performed by either PEI or Lipofectamine 2000 (Invitrogen) reagents with a DNA:PEI/Lipofectamine 2000 ratio of 1:3 or 1:2. Transfected cells were incubated in 60 mm culture dishes for 48 h and fed with 10% FBS and DMEM. Following lysis with either Reporter Lysis 5X Buffer (Promega) or radioimmunoprecipitation assay buffer, assays for reporter activity (luciferase assay, Promega) as well as for protein concentration (Bradford assay, Bio-Rad) were carried out. β -galactosidase was measured using the Galacto-Light Plus reagents (Tropix Inc) as an internal normalizer. All luciferase activities were normalized to β -galactosidase activity and are shown as mean-fold differences relative to empty luciferase plasmids and are shown as mean \pm SEM.

Lentiviral production and stable cell line establishment

HEK 293T cells were seeded in a 100 mm cell culture dish followed by PEI transfection with pMD2.G, psPAX2 and *PMIS-EV*, *PMIS-miR-23a*, *PMIS-miR-24*, *PITX2*, or *NSD2* expression plasmids. The medium was changed 24 h post transfection and lentivirus-containing medium was collected at 48 h, 72 h, and 96 h post transfection and filtered through a 0.45 μ m polyvinylidene fluoride filter. LS-8 cells were seeded in 100 mm cell culture dishes. After 24 h, the medium was aspirated and replaced by lentiviral-containing medium with 8 μ g/ml polybrene. Medium was changed to normal culture medium after 24 h. Transduced cells were either selected through puromycin (1 μ g/ml) selection, G418 (5 mg/ml) selection or cell sorting. For cell sorting, the cells were trypsinized, washed and resuspended with PBS, and filtered through a 70 μ m nylon mesh strainer. The GFP⁺ cell populations were sorted through either Becton Dickinson FACS Aria II or FACS Fusion cell sorters. The sorted cells were then cultured in normal cell culture medium for stable cell line expansion.

MTT assay

LS8 or LS8-NSD2 cells were seeded in triplicates for each assay time points in 96-well plates at 20,000 cells/well and

Table 1
List of antibodies for immunofluorescence

| Antibodies | Manufacturer | Working Dilution |
|---|----------------|------------------|
| Anti-WHSC1/NSD2 mouse antibody (29D1) ab75359 | Abcam | 1:50 |
| Anti-PITX2 sheep antibody AF7388 | R&D Systems | 1:50 |
| Anti-LEF-1 rabbit antibody 22305 | Cell Signaling | 1:50 |
| Anti-GLI-1 rabbit antibody ab49314 | Abcam | 1:50 |
| Anti-SOX2 goat antibody AF2018 | R&D Systems | 1:50 |

Whsc1 regulates gene expression during development

Table 2

List of primers used for quantitative RT-PCR

| Gene | Forward primer (5'-3') | Reverse primer (5'-3') |
|--------------|----------------------------------|----------------------------|
| β-Actin | CTCTTCCAGCCTTCCTTC | ATCTCCTTCTGCATCCTGTC |
| Whsc1 | TGCCAAAAAGGAGTACGTGTG | CTTCGGGAAAGTCCAAGGCAG |
| Pitx2 | CTGGAAGCCACTTTCAGAG | AAGCCATTCTTGACAGCTC |
| PMIS-miR-23a | CTAAGGAAATCCTGATCAGCAATGTGAT | GTCAGCTCTTAGTATTTCATGAGATG |
| PMIS-miR-24 | CTAACTGTTCTCTGCTGATCAAAGTACGACCA | GTCAGCTCTTAGTATTTCATGAGATG |

cultured in DMEM (10% FBS and 1% penicillin/streptomycin). MTT assay was performed at 6 h, 24 h, and 48 h post seeding. For each MTT assay, media were discarded from cell cultures and 50 µl of serum-free media and 50 µl of MTT solution (5 mg/ml in PBS) were placed into each well. Plates were incubated for 3 h at 37 °C. After incubation, 150 µl MTT reagent (4 mM HCl, 0.1% NP40 in isopropanol) was added to each well. The plate was then wrapped with foil and shaken on an orbital shaker for 15 min after which the absorbance was read at 620 nm.

Cell counting assay

LS8 or LS8-NSD2 cells were seeded in quadruplicates for each harvesting time points in 60 mm dishes at 10^5 cells/dish and cultured with DMEM (10% FBS and 1% penicillin/streptomycin). Cells were trypsinized and suspended with 1.5 to 2.5 ml culture medium, followed by cell counting using a hemocytometer at 24 h, 48 h, 72 h, 96 h, and 120 h post seeding.

Real-time quantitative reverse transcription PCR

Total RNA was isolated from cells or mouse mandible tissues using miRNeasy Mini Kit (Qiagen) or standard RNA preparation protocol. Reverse transcription and quantitative real-time PCR for microRNA detection were carried out with miScript PCR system (Qiagen) according to the manufacturer's protocol. Reverse transcription and quantitative real-time PCR for mRNAs were performed using a TaKaRa kit (TaKaRa, RR036A, RR420L). All Ct numbers were below 35 cycles. PCR products were examined by melting curve analysis and the sequences were confirmed. Fold change was calculated using the $2^{-\Delta\Delta CT}$ method. The primers used for qPCR are listed in Table 2. The primers

Table 3

List of antibodies used for Western blot assays

| Antibody Name | Manufacturer | Working Dilution |
|--|--------------------------|------------------|
| Anti-PITX2 ^{ABC} antibody PA1020 | Capra Science | (WB) 1:2000 |
| Anti-WHSC1/NSD2 mouse antibody [29D1] ab75359 | Abcam | (WB) 1:2000 |
| Anti-GAPDH mouse antibody sc32233 | Santa Cruz Biotechnology | (WB) 1:10,000 |
| Anti-Histone 3 rabbit antibody 9715 | Cell Signaling | (WB) 1:2000 |
| Anti-Histone H3 (mono methyl K36) rabbit antibody ab9048 | Abcam | (WB) 1:2000 |

used to detect *miR-23a/b-3p* and *miR-24-1/2* were purchased from Qiagen.

Western blot assays

Cell lysates from LS-8, HEK 293 cells and stable cell lines were analyzed on 4% stacking gel and 10 to 15% SDS-PAGE separating gels. Following electrophoresis, the protein was transferred to polyvinylidene fluoride membranes (Millipore), immunoblotted, and detected with a horseradish peroxidase-conjugated secondary antibody and Clarity Western ECL Blotting Substrate (Bio-Rad). The following antibodies were used to detect the proteins (Table 3).

Chromatin immunoprecipitation assay

ChIP assays were performed as previously described (33) using the ChIP Assay Kit (Zymo research). LS-8 cells were cross-linked in 1% formaldehyde at room temp for 7 min. Cross-linked cells were sonicated three times (6 s duration for each round, 25% of maximum amplitude) to shear the genomic DNA in to 200 to 1000 bp fragments. Then the DNA/protein complexes were immunoprecipitated with 5 µg PITX2 antibody (Capra Science), WHSC1 and H3K36me2 (Abcam) antibodies or 5 µg rabbit IgG as control. Precipitated DNAs were subjected to PCR to evaluate the enrichment of Pitx2 binding. The primers used for PCR are listed in Table 4. All the PCR products were analyzed on a 1.5% agarose gel for the correct size and confirmed by sequencing.

miRNA microarray

Incisor and molar tooth germs were dissected from P0 and P10 mice using a dissection microscope. To separate epithelium and mesenchyme, the tooth germs were treated with Dispase II and Collagenase I (Worthington) for 30 min at 37 °C. This procedure separates the epithelium from the mesenchyme and allows for specific RNA extraction of the two tissue types (37). Total RNAs including microRNA were prepared using miRNeasy Mini Kit from Qiagen. LC Sciences performed the miRNA microarray analyses.

Statistical analysis

All quantified results are presented as mean ± SEM, and with an N value indicating the number of biological replicates. A two-tailed unpaired Student's *t* test and either one- or two-way ANOVA were used to determine statistical significance.

Table 4
List of primers used for ChIP-PCR assay

| ChIP primers | Forward primer (5'-3') | Reverse primer (5'-3') |
|------------------------------|------------------------|---------------------------|
| Whsc1 (Pitx2)-1 | GAGCGATTCTCCTGCCTCAGCC | CACTTTGGGAGGCTGAGGCG |
| Whsc1 (con)-1 | GGTGACTGTTGTTGTCCATAGC | GGTGGGAAGAGTTAAGCATCAC |
| Whsc1 (Pitx2)-2 | ACATGTCTGCTGGTAACAAC | CTAAAACCTCAAAGGGCTTGC |
| Whsc1 (con)-2 | AACTCTGCACTTGGCAGGAA | TTGGCTTTGTGGGCGATGTA |
| Pitx2 (Pitx2) | TTCTGCCGATCCTTGTGGAC | TTCTGCCGATCCTTGTGGAC |
| Pitx2 (con) | TGGTCTTCAGCACCAAAGCG | TATTAGCCGGTAGCCCCAAC |
| pre-miR-23a-27a-24-2 (Pitx2) | TCCTGCCCTAACCTGTCAAG | AGCTAAGGACCCCAACCGACT |
| pre-miR-23a-27a-24-2 (con) | GCCTCCCTGTTTGTATGTCTC | CAGCTGGTTTCTGTGCATGCTC |
| pre-miR-23b-27b-24-1 (Pitx2) | GAGCTGAGACCTGCTCATCC | GGTGACTGACTGTCTGTGC |
| pre-miR-23b-27b-24-1 (con) | TGTTGTGTGTGATGTTAAAGGA | CAGCTTCTTTCTGTGTCATGAT |
| Amelogenin (Pitx2) | GACTGCCTTTTAGTTCATTCTC | TCTGTGATCCATATTTACACACCTG |
| Amelogenin (con) | CAGATCTTATTGCGACCTGA | AAAAGACATCTGCCCTCTTCT |
| Sox2 (Pitx2) | GAGCTTCTTTCCGTTGATGC | TTCCCTACTCCACCAACCTG |
| Sox2 (con) | TGGTCTTCAGCACCAAAGCG | TATTAGCCGGTAGCCCCAAC |

Data availability

All data are available in the main article or the [supporting information](#).

Supporting information—This article contains supporting information.

Acknowledgments—We thank members of the Amendt lab for their expertise and helpful discussions and previous lab members for contributing to the study. We also thank the Iowa Institute of Human Genetics (IIHG) Genomics Division for their help with sequencing, and the Flow Cytometry core for cell sorting to establish our stable cell lines.

Author contributions—D. S. and B. A. A. conceptualization; D. S., S. E., and F. S. investigation; D. S., S. E., Z. S., and F. S. methodology; D. S., S. E., F. S., and B. A. A. formal analysis; D. S. and S. E., validation; D. S. writing—original draft; B. A. A. writing—review and editing; B. A. A. resources; B. A. A. funding acquisition.

Funding and additional information—This work was supported by a grant from the National Institute of Health (DE028527) and funding from the University of Iowa.

Conflict of interest—B. A. A. is the CEO of NaturemiRI. LLC.

Abbreviations—The abbreviations used are: ARS, Axenfeld-Rieger syndrome; ChIP, chromatin immunoprecipitation; DESC, dental epithelial stem cells; DM, dental mesenchyme; DMEM, Dulbecco's modified Eagle's medium; FBS, fetal bovine serum; LaCL, labial cervical loop; MTT, 3-(4,5-dimethylthiazol-2-yl)-2,5-diphenyl-2H-tetrazolium bromide; PMIS, plasmid-based miRNA inhibition system; RT-qPCR, real-time quantitative reverse transcription PCR; TF, transcription factor; WHS, Wolf-Hirschhorn syndrome; WHSC, Wolf-Hirschhorn syndrome candidate.

References

- Hirschhorn, K., Cooper, H. L., and Firschein, I. L. (1965) Deletion of short arms of chromosome 4-5 in a child with defects of midline fusion. *Humangenetik* **1**, 479–482
- Wolf, U., Reinwein, H., Porsch, R., Schröter, R., and Baitsch, H. (1965) Defizienz an den kurzen armen eines chromosomes Nr. 4. *Humangenetik* **1**, 397–413
- Lurie, I. W., Lazjuk, G. I., Usaova, Y. I., Presman, E. B., and Gurevich, D. B. (1980) The Wolf-Hirschhorn syndrome. *Clin. Genet.* **17**, 375–384
- Shannon, N. L., Maltby, E. L., Rigby, A. S., and Quarrell, O. W. (2001) An epidemiological study of Wolf-Hirschhorn syndrome: life expectancy and cause of mortality. *J. Med. Genet.* **38**, 674–679
- Battaglia, A., Carey, J. C., and South, S. T. (2015) Wolf-Hirschhorn syndrome: a review and update. *Am. J. Med. Genet. C Semin. Med. Genet.* **169**, 216–223
- Shimizu, K., Wakui, K., Kosho, T., Okamoto, N., Mizuno, S., Itomi, K., et al. (2014) Microarray and FISH-based genotype-phenotype analysis of 22 Japanese patients with Wolf-Hirschhorn syndrome. *Am. J. Med. Genet. A.* **164a**, 597–609
- Yamamoto-Shimajima, K., Kouwaki, M., Kawashima, Y., Itomi, K., Momosaki, K., Ozasa, S., et al. (2019) Natural histories of patients with Wolf-Hirschhorn syndrome derived from variable chromosomal abnormalities. *Congenit. Anom. (Kyoto)* **59**, 169–173
- Zollino, M., Murdolo, M., Marangi, G., Pecile, V., Galasso, C., Mazzanti, L., et al. (2008) On the nosology and pathogenesis of Wolf-Hirschhorn syndrome: genotype-phenotype correlation analysis of 80 patients and literature review. *Am. J. Med. Genet. C Semin. Med. Genet.* **148c**, 257–269
- Battaglia, A., Filippi, T., and Carey, J. C. (2008) Update on the clinical features and natural history of Wolf-Hirschhorn (4p-) syndrome: experience with 87 patients and recommendations for routine health supervision. *Am. J. Med. Genet. C Semin. Med. Genet.* **148c**, 246–251
- Limeres, J., Serrano, C., De Nova, J. M., Silvestre-Rangil, J., Machuca, G., Maura, I., et al. (2020) Oral manifestations of Wolf-Hirschhorn syndrome: genotype-phenotype correlation analysis. *J. Clin. Med.* **9**, 3556
- Babich, S. B., Banducci, C., and Teplitsky, P. (2004) Dental characteristics of the Wolf-Hirschhorn syndrome: a case report. *Spec. Care Dentist.* **24**, 229–231
- Kuo, A. J., Cheung, P., Chen, K., Zee, B. M., Kioi, M., Luring, J., et al. (2011) NSD2 links dimethylation of histone H3 at lysine 36 to oncogenic programming. *Mol. Cell* **44**, 609–620
- Huang, C., and Zhu, B. (2018) Roles of H3K36-specific histone methyltransferases in transcription: antagonizing silencing and safeguarding transcription fidelity. *Biophys. Rep.* **4**, 170–177
- Li, Y., Trojer, P., Xu, C. F., Cheung, P., Kuo, A., Drury, W. J., 3rd, et al. (2009) The target of the NSD family of histone lysine methyltransferases depends on the nature of the substrate. *J. Biol. Chem.* **284**, 34283–34295
- Nimura, K., Ura, K., Shiratori, H., Ikawa, M., Okabe, M., Schwartz, R. J., et al. (2009) A histone H3 lysine 36 trimethyltransferase links Nkx2-5 to Wolf-Hirschhorn syndrome. *Nature* **460**, 287–291
- Bergemann, A. D., Cole, F., and Hirschhorn, K. (2005) The etiology of Wolf-Hirschhorn syndrome. *Trends Genet.* **21**, 188–195
- Barrie, E. S., Alfaro, M. P., Pfau, R. B., Goff, M. J., McBride, K. L., Manickam, K., et al. (2019) De novo loss-of-function variants in NSD2 (WHSC1) associate with a subset of Wolf-Hirschhorn syndrome. *Cold Spring Harb. Mol. Case Stud.* **5**, a004044
- Boczek, N. J., Lahner, C. A., Nguyen, T. M., Ferber, M. J., Hasadsri, L., Thorland, E. C., et al. (2018) Developmental delay and failure to thrive associated with a loss-of-function variant in WHSC1 (NSD2). *Am. J. Med. Genet. A* **176**, 2798–2802

Whsc1 regulates gene expression during development

19. Lozier, E. R., Kononov, F. A., Kanivets, I. V., Pyankov, D. V., Koshkin, P. A., Baleva, L. S., *et al.* (2018) De novo nonsense mutation in WHSC1 (NSD2) in patient with intellectual disability and dysmorphic features. *J. Hum. Genet.* **63**, 919–922
20. Lee, Y. F., Nimura, K., Lo, W. N., Saga, K., and Kaneda, Y. (2014) Histone H3 lysine 36 methyltransferase Whsc1 promotes the association of Runx2 and p300 in the activation of bone-related genes. *PLoS One* **9**, e106661
21. Thesleff, I. (2003) Epithelial-mesenchymal signalling regulating tooth morphogenesis. *J. Cell Sci.* **116**, 1647–1648
22. Gulabivala, K., and Ng, Y. L. (2014) 1 - tooth organogenesis, morphology and physiology. In: Gulabivala, K., Ng, Y.-L., eds. *Endodontics*, Fourth Edition, Mosby/Elsevier, Edinburgh: 2–32
23. Amendt, B. A., Sutherland, L. B., Semina, E., and Russo, A. F. (1998) The molecular basis of rieger syndrome: analysis of Pitx2 homeodomain protein activities. *J. Biol. Chem.* **273**, 20066–20072
24. Semina, E. V., Reiter, R., Laysens, N. J., Alward, L. M., Small, K. W., Datson, N. A., *et al.* (1996) Cloning and characterization of a novel bicoid-related homeobox transcription factor gene, RIEG, involved in Rieger syndrome. *Nat. Genet.* **14**, 392–399
25. Gage, P. J., Suh, H., and Camper, S. A. (1999a) The bicoid-related Pitx gene family in development. *Mamm. Genome* **10**, 197–200
26. Lin, C. R., Kioussi, C., O'Connell, S., Briata, P., Szeto, D., Liu, F., *et al.* (1999) Pitx2 regulates lung asymmetry, cardiac positioning and pituitary and tooth morphogenesis. *Nature* **401**, 279–282
27. Lu, M., Pressman, C., Dyer, R., Johnson, R. L., and Martin, J. F. (1999a) Function of Rieger syndrome gene in left-right asymmetry and craniofacial development. *Nature* **401**, 276–278
28. Wang, J., Saadi, I., Wang, J., Engel, J. J., Kaburas, A., Russo, A. F., *et al.* (2013) PIAS1 and PIASy differentially regulate PITX2 transcriptional activities. *J. Biol. Chem.* **288**, 12580–12595
29. Pispas, J., and Thesleff, I. (2003) Mechanisms of ectodermal organogenesis. *Dev. Biol.* **262**, 195–205
30. Tucker, A., and Sharpe, P. (2004) The cutting-edge of mammalian development; how the embryo makes teeth. *Nat. Rev. Genet.* **5**, 499–508
31. Vadlamudi, U., Espinoza, H. M., Ganga, M., Martin, D. M., Liu, X., Engelhardt, J. F., *et al.* (2005) PITX2, β -catenin, and LEF-1 interact to synergistically regulate the LEF-1 promoter. *J. Cell Sci.* **118**, 1129–1137
32. Amen, M., Liu, X., Vadlamudi, U., Elizondo, G., Diamond, E., Engelhardt, J. F., *et al.* (2007) PITX2 and β -catenin interactions regulate Lef-1 isoform expression. *Mol. Cell. Biol.* **27**, 7560–7573
33. Sun, Z., Yu, W., Navarro, M. S., Sweat, M., Eliason, S., Sharp, T., *et al.* (2016) Sox2 and Lef-1 interact with Pitx2 to regulate incisor development and stem cell renewal. *Development* **143**, 4115–4126
34. Sweat, Y. Y., Sweat, M., Yu, W., Sanz-Navarro, M., Zhang, L., Sun, Z., *et al.* (2020) Sox2 controls Periderm and Rugae development to inhibit oral Adhesions. *J. Dent. Res.* **99**, 1397–1405
35. Bartel, D. P. (2004) MicroRNAs: genomics, biogenesis, mechanism, and function. *Cell* **116**, 281–297
36. Du, T., and Zamore, P. D. (2007) Beginning to understand microRNA function. *Cell Res.* **17**, 661–663
37. Cao, H., Wang, J., Li, X., Florez, S., Huang, Z., Venugopalan, S. R., *et al.* (2010) MicroRNAs play a critical role in tooth development. *J. Dent. Res.* **89**, 779–784
38. Oommen, S., Otsuka-Tanaka, Y., Imam, N., Kawasaki, M., Kawasaki, K., Jalani-Ghazani, F., *et al.* (2012) Distinct roles of microRNAs in epithelium and mesenchyme during tooth development. *Dev. Dyn.* **241**, 1465–1472
39. Sayed, D., and Abdellatif, M. (2011) MicroRNAs in development and disease. *Physiol. Rev.* **91**, 827–887
40. Ivey, K. N., and Srivastava, D. (2015) microRNAs as developmental regulators. *Cold Spring Harb. Perspect. Biol.* **7**, a008144
41. Su, D., Krongbamee, T., Sun, H., Hong, L., and Amendt, B. A. (2022) Exploring craniofacial and dental development with microRNAs. *Biochem. Soc. Trans.* **50**, 1897–1909
42. Hassan, M. Q., Gordon, J. A., Beloti, M. M., Croce, C. M., van Wijnen, A. J., Stein, J. L., *et al.* (2010) A network connecting Runx2, SATB2, and the miR-23a~27a~24-2 cluster regulates the osteoblast differentiation program. *Proc. Natl. Acad. Sci. U. S. A.* **107**, 19879–19884
43. Godfrey, T. C., Wildman, B. J., Beloti, M. M., Kemper, A. G., Ferraz, E. P., Roy, B., *et al.* (2018) The microRNA-23a cluster regulates the developmental HoxA cluster function during osteoblast differentiation. *J. Biol. Chem.* **293**, 17646–17660
44. Zeng, H. C., Bae, Y., Dawson, B. C., Chen, Y., Bertin, T., Munivez, E., *et al.* (2017) MicroRNA miR-23a cluster promotes osteocyte differentiation by regulating TGF- β signalling in osteoblasts. *Nat. Commun.* **8**, 15000
45. Shen, Y., Li, Y., Ye, F., Wang, F., Wan, X., Lu, W., *et al.* (2011) Identification of miR-23a as a novel microRNA normalizer for relative quantification in human uterine cervical tissues. *Exp. Mol. Med.* **43**, 358–366
46. Chen, Q., Xu, J., Li, L., Li, H., Mao, S., Zhang, F., *et al.* (2014) MicroRNA-23a/b and microRNA-27a/b suppress Apaf-1 protein and alleviate hypoxia-induced neuronal apoptosis. *Cell Death Dis.* **5**, e1132
47. Gao, P., Tchernyshyov, I., Chang, T. C., Lee, Y. S., Kita, K., Ochi, T., *et al.* (2009) c-Myc suppression of miR-23a/b enhances mitochondrial glutamine expression and glutamine metabolism. *Nature* **458**, 762–765
48. Viswanathan, V., Damle, S., Zhang, T., Opendaker, L., Modarai, S., Accerbi, M., *et al.* (2017) An miRNA expression signature for the human colonic stem cell niche distinguishes malignant from normal epithelia. *Cancer Res.* **77**, 3778–3790
49. Li, A., Song, T., Wang, F., Liu, D., Fan, Z., Zhang, C., *et al.* (2012) MicroRNAome and expression profile of developing tooth germ in miniature pigs. *PLoS One* **7**, e52256
50. Eliason, S., Su, D., Pinho, F., Sun, Z., Zhang, Z., Li, X., *et al.* (2022) HMGN2 represses gene transcription via interaction with transcription factors Lef-1 and Pitx2 during amelogenesis. *J. Biol. Chem.* **298**, 102295
51. Jernvall, J., Kettunen, P., Karavanova, I., Martin, L. B., and Thesleff, I. (1994) Evidence for the role of the enamel knot as a control center in mammalian tooth cusp formation: non-dividing cells express growth stimulating Fgf-4 gene. *Int. J. Dev. Biol.* **38**, 463–469
52. Jernvall, J., Aberg, T., Kettunen, P., Keränen, S., and Thesleff, I. (1998) The life history of an embryonic signaling center: BMP-4 induces p21 and is associated with apoptosis in the mouse tooth enamel knot. *Development* **125**, 161–169
53. Kwon, H.-J., Yoon, K.-S., and Jung, H.-S. (2013) Expression patterns of Ki-67, cyclin A, and cyclin D1 during tooth development. *Korean J. Phys. Anthropol.* **26**, 41–49
54. Nakagawa, E., Zhang, L., Shin, J.-O., Kim, E.-J., Cho, S.-W., Ohshima, H., *et al.* (2012) The novel expression of Oct3/4 and Bmi1 in the root development of mouse molars. *Cell Tissue Res.* **347**, 479–484
55. Pandolfi, S., and Stecca, B. (2015) Cooperative integration between HEDGEHOG-GLI signalling and other oncogenic pathways: implications for cancer therapy. *Expert Rev. Mol. Med.* **17**, e5
56. Ishikawa, Y., Ida-Yonemochi, H., Saito, K., Nakatomi, M., and Ohshima, H. (2021) The sonic Hedgehog–Patched–Gli signaling pathway maintains dental epithelial and pulp stem/progenitor cells and regulates the function of odontoblasts. *Front. Dent. Med.* **2**, 651334
57. Cao, H., Florez, S., Amen, M., Huynh, T., Skobe, Z., Baldini, A., *et al.* (2010) Tbx1 regulates progenitor cell proliferation in the dental epithelium by modulating Pitx2 activation of p21. *Dev. Biol.* **347**, 289–300
58. Karlic, R., Chung, H. R., Lasserre, J., Vlahovicek, K., and Vingron, M. (2010) Histone modification levels are predictive for gene expression. *Proc. Nat. Acad. Sci. U. S. A.* **107**, 2926–2931
59. Maunakea, A. K., Nagarajan, R. P., Bilenky, M., Ballinger, T. J., D'Souza, C., Fouse, S. D., *et al.* (2010) Conserved role of intragenic DNA methylation in regulating alternative promoters. *Nature* **466**, 253–257
60. Xiao, S., Xie, D., Cao, X., Yu, P., Xing, X., Chen, C.-C., *et al.* (2012) Comparative epigenomic annotation of regulatory DNA. *Cell* **149**, 1381–1392
61. Rada-Iglesias, A., Bajpai, R., Prescott, S., Brugmann, S. A., Swigut, T., and Wysocka, J. (2012) Epigenomic annotation of enhancers predicts transcriptional regulators of human Neural crest. *Cell Stem Cell* **11**, 633–648
62. Mill, J., and Heijmans, B. T. (2013) From promises to practical strategies in epigenetic epidemiology. *Nat. Rev. Genet.* **14**, 585–594
63. Martinez, N. J., and Gregory, R. I. (2010) MicroRNA gene regulatory pathways in the establishment and maintenance of ESC identity. *Cell Stem Cell* **7**, 31–35

64. Nieminen, P., Kotilainen, J., Aalto, Y., Knuutila, S., Pirinen, S., and The-sleff, I. (2003) MSX1 gene is deleted in Wolf-Hirschhorn syndrome pa-tients with oligodontia. *J. Dent. Res.* **82**, 1013–1017
65. Maas, N. M., Van Buggenhout, G., Hannes, F., Thienpont, B., Sanlaville, D., Kok, K., *et al.* (2008) Genotype-phenotype correlation in 21 patients with Wolf-Hirschhorn syndrome using high resolution array comparative genome hybridisation (CGH). *J. Med. Genet.* **45**, 71–80
66. Gavril, E.-C., Luca, A. C., Curpan, A.-S., Popescu, R., Resmerita, I., Panzaru, M. C., *et al.* (2021) Wolf-hirschhorn syndrome: clinical and genetic study of 7 new cases, and Mini review. *Children (Basel)* **8**, 751
67. Lesot, H., Vonesch, J. L., Peterka, M., Turecková, J., Peterková, R., and Ruch, J. V. (1996) Mouse molar morphogenesis revisited by three-dimensional reconstruction. II. Spatial distribution of mitoses and apoptosis in cap to bell staged first and second upper molar teeth. *Int. J. Dev. Biol.* **40**, 1017–1031
68. Peterková, R., Peterka, M., and Lesot, H. (2003) The developing mouse dentition: a new tool for apoptosis study. *Ann. N. Y Acad. Sci.* **1010**, 453–466
69. Dai, J., Jiang, L., Qiu, L., Shao, Y., Shi, P., and Li, J. (2020) WHSC1 promotes cell proliferation, migration, and invasion in hepatocellular carcinoma by activating mTORC1 signaling. *Oncotargets Ther.* **13**, 7033–7044
70. Kojima, M., Sone, K., Oda, K., Hamamoto, R., Kaneko, S., Oki, S., *et al.* (2019) The histone methyltransferase WHSC1 is regulated by EZH2 and is important for ovarian clear cell carcinoma cell proliferation. *BMC Cancer* **19**, 455
71. Liu, C., Jiang, Y.-H., Zhao, Z.-L., Wu, H.-W., Zhang, L., Yang, Z., *et al.* (2019) Knockdown of histone methyltransferase WHSC1 induces apoptosis and inhibits cell proliferation and Tumorigenesis in Salivary Adenoid Cystic carcinoma. *Anticancer Res.* **39**, 2729–2737
72. Hock, R., Furusawa, T., Ueda, T., and Bustin, M. (2006) HMG chromo-somal proteins in development and disease. *Trends. Cell Biol.* **17**, 72–79
73. Amendt, B. A., Sutherland, L. B., and Russo, A. F. (1999) Multifunctional role of the Pitx2 homeodomain protein C-terminal tail. *Mol. Cell. Biol.* **19**, 7001–7010
74. Acharya, M., Sharp, M. W., Mirzayans, F., Footz, T., Huang, L., Birdi, C., *et al.* (2012) Yeast two-hybrid analysis of a human trabecular meshwork cDNA library identified EFEMP2 as a novel PITX2 interacting protein. *Mol. Vis.* **18**, 2182–2189
75. Acharya, M., Lingenfelter, D. J., Huang, L., Gage, P. J., and Walter, M. A. (2009) Human PRKC apoptosis WT1 regulator is a novel PITX2-interacting protein that regulates PITX2 transcriptional activity in Ocular cells*. *J. Biol. Chem.* **284**, 34829–34838
76. Venugopalan, S. R., Amen, M. A., Wang, J., Wong, L., Cavender, A. C., D'Souza, R. N., *et al.* (2008) Novel expression and transcriptional regu-lation of FoxJ1 during oro-facial morphogenesis. *Hum. Mol. Genet.* **17**, 3643–3654
77. Amen, M., Espinoza, H. M., Cox, C., Liang, X., Wang, J., Link, T. M., *et al.* (2008) Chromatin-associated HMG-17 is a major regulator of homeo-domain transcription factor activity modulated by Wnt/beta-catenin signaling. *Nucleic Acids Res.* **36**, 462–476
78. Cox, C. J., Espinoza, H. M., McWilliams, B., Chappell, K., Morton, L., Hjalt, T. A., *et al.* (2002) Differential regulation of gene expression by PITX2 isoforms. *J. Biol. Chem.* **277**, 25001–25010
79. Green, P. D., Hjalt, T. A., Kirk, D. E., Sutherland, L. B., Thomas, B. L., Sharpe, P. T., *et al.* (2001) Antagonistic regulation of Dlx2 expression by PITX2 and Msx2: implications for tooth development. *Gene Expr.* **9**, 265–281
80. Jaffe, J. D., Wang, Y., Chan, H. M., Zhang, J., Huether, R., Kryukov, G. V., *et al.* (2013) Global chromatin profiling reveals NSD2 muta-tions in pediatric acute lymphoblastic leukemia. *Nat. Genet.* **45**, 1386–1391
81. Cao, H., Yu, W., Li, X., Wang, J., Gao, S., Holton, N. E., *et al.* (2016) A new plasmid-based microRNA inhibitor system that inhibits micro-RNA families in transgenic mice and cells: a potential new therapeutic reagent. *Gene Ther.* **23**, 527–542
82. Chen, L. S., Couwenhoven, R. I., Hsu, D., Luo, W., and Snead, M. L. (1992) Maintenance of Amelogenin gene expression by transformed epithelial cells of mouse enamel organ. *Arch. Oral Biol.* **37**, 771–778